PNAS

Supplementary Information

Universal open MHC-I molecules for rapid peptide loading and enhanced complex stability across HLA allotypes.

[1,2]Yi Sun†, [1,2]Michael C. Young†, [1,2]Claire H. Woodward†, [1,2]Julia N. Danon, [3]Hau V. Truong, [1,2]Sagar Gupta, [2]Trenton J. Winters, [4]Joan Font-Burgada, [2,3]George M. Burslem, and [1,2]Nikolaos G. Sgourakis*

[1]Center for Computational and Genomic Medicine, Department of Pathology and Laboratory Medicine, The Children's Hospital of Philadelphia, Philadelphia, PA, 19104, USA
[2]Department of Biochemistry and Biophysics, Perelman School of Medicine, University of Pennsylvania, 3401 Civic Center Blvd, Philadelphia, PA, 19104, USA
[3]Department of Cancer Biology and Epigenetics Institute, Perelman School of Medicine, University of Pennsylvania, Philadelphia, PA, 19104, USA
[4]Cancer Signaling and Microenvironment Program, Fox Chase Cancer Center, Philadelphia, PA, 19111, USA

†Contributed equally to this work.

***Correspondence**: Nikolaos G. Sgourakis
Email: Nikolaos.Sgourakis@Pennmedicine.upenn.edu

This PDF file includes:

Supplemental Methods

Peptides and ligands. All peptide sequences are given as standard single-letter codes. Peptides for different HLA allotypes were selected by NetMHCpan4.1(1) and purchased from Genscript, Piscataway, USA, at >90% purity. L-β-Phenylalanine (βF) containing placeholder peptides were synthesized in-house on 2-chlorotrityl resin using a CEM Liberty Blue automated microwave peptide synthesizer from Fmoc protected amino acids (including Fmoc-β-Phe-OH) employing iterative cycles of N, N'-Diisopropylcarbodiimide (DIC)/Ethyl cyanohydroxyiminoacetate (Oxyma) mediated coupling and piperidine mediated deprotection, both under microwave irradiation. Peptides were deprotected and cleaved from the resin by treatment with trifluoroacetic acid/water/triisoproylsilane/phenol (88:5:5:2) for 1-3 hours. The solvent was removed under a flow of nitrogen, and peptides were precipitated with ice-cold ether. Peptides were subsequently purified by reverse phase chromatography eluting with 5-95% acetonitrile in water containing 0.05% trifluoroacetic acid over a C18 column. Peaks containing peptides were identified by LC-MS, pooled, and concentrated in vacuo to yield a colorless solid. Photosensitive peptides were purchased from Biopeptek Inc, Malvern, USA, or synthesized in-house using Fmoc-3-amino-3-(2-nitrophenyl)-propionic acid (J). Peptides were solubilized in distilled water and centrifuged at 14000 rpm for 15 minutes. The concentration of each peptide solution was measured and calculated using the respective absorbance and extinction coefficient at 205 nm wavelength. MR1 C262S ligand acetyl-6-formylpterin (Ac-6-FP) and diclofenac (DCF) were purchased from Cayman Chemical (#23303) and Sigma D6899-10G.

TCGA peptide selection. The 1018 putative driver mutations used in Marty et al. (pmid: 29107334) were selected to produce all possible 8-11-mer peptides containing each mutation and screened for HLA-A02:01 binding with NetMHCPan4.0. A cutoff of 400 nM predicted affinity was applied, and remaining peptides were ranked by mutation frequency across TCGA patients. The top 50 ranked peptides were selected for the study.

Recombinant protein expression, refolding, and purification. Plasmid DNA encoding the BirA Substrate Peptide (BSP, LHHILDAQKMVWNHR)-tagged luminal domain of MHC-I heavy chains and human β_2m were provided by the NIH tetramer facility (Emory University) and transformed into *Escherichia coli* BL21(DE3) cells (New England Biolabs). Open heavy chains (G120C) and β_2m (H31C) were generated using site-directed mutagenesis and transformed into *Escherichia coli* BL21(DE3) cells using the pET-22b(+) vector. Cells were grown and harvested in the Luria-Broth medium, and inclusion bodies were pelleted and purified as previously described(2). For the generation of pMHC-I molecules, *in vitro* refolding was performed by slowly diluting a 100 mg mixture of either wild type (WT) or open MHC-I and β_2m at a 1:3 molar ratio over 4 hours in refolding buffer (0.4 M L-Arginine HCl, 100 mM Tris pH 8, 2 mM EDTA, 5 mM reduced L-glutathione, 0.5 mM oxidized L-glutathione) supplemented with 10 mg of the peptide. The mixture was protected from light when refolded with photosensitive peptides. Refolding proceeded for 4

days, and proteins were purified by size exclusion chromatography (SEC) using a HiLoad 16/600 Superdex 75 pg column at 1 mL/min with 150 mM NaCl, 20 mM Tris buffer, pH 8.0. Purified proteins were further confirmed in reduced and non-reduced conditions using sodium dodecyl sulfate-polyacrylamide (SDS-PAGE) gel electrophoresis. MR1 refolding was performed by diluting a 90 mg mixture of either WT or open HC and β_2m at a 1:1.3 molar ratio overnight in refolding buffer supplemented with 5 mg of DCF or Ac-6-FP. Protein purification was performed as described above.

Differential Scanning Fluorimetry. Differential Scanning Fluorimetry (DSF) was used to assess the thermal stabilities of the WT and the open pMHC-I protein complexes. 7 µM of placeholder peptide-loaded MHC-I molecules were incubated with the desired peptide at a 1:10 molar ratio at room temperature (RT) overnight and then mixed with 10X SYPRO Orange dye in PBS buffer (150 mM NaCl, 20 mM sodium phosphate, pH 7.2) to a final volume of 20 µL. Samples were loaded into MicroAmp Optical 384 well plate and ran in triplicates. The experiment was performed on a QuantStudio™ 5 Real-Time PCR machine with excitation and emission wavelengths set to 470 nm and 569 nm. The temperature was incrementally increased at a rate of 1°C per minute between 25°C and 95°C. Data analysis and fitting were performed in GraphPad Prism v9. To determine the percent unfolding, WT and open HLA-A*02:01/KILGFVFJV were UV irradiated for 0, 10, 20, 30, 40, 50, and 60 minutes. The full DSF traces were recorded at a constant rate of 1°C per minute between 25°C and 95°C. The fluorescence intensity (I) at 25°C was then normalized against the maximum I. Data analysis and fitting were performed in GraphPad Prism v9.

NMR sample preparation and backbone resonance assignment. NMR samples of WT and open HLA-A*02:01/β_2m/MART1 complex were prepared with an [^{15}N, ^{13}C, ^{2}H] isotope-selective labeling scheme using established protocols and reagents(3, 4). The HC and β_2m components were each isotopically labeled independently using M9 media in *E. coli*(13) and refolded with the complementary complex components expressed at natural isotopic abundance, as described previously for the same system, to generate two NMR samples each for open and WT. Samples in the concentration range of 50 to 150 µM were prepared in a standard NMR buffer (150 mM NaCl, 20 mM sodium phosphate pH 7.2, 0.001 M sodium azide, 5% D_2O) in the presence of 2-fold molar excess of MART1 peptide, and all datasets were collected at 298-300 K. Backbone resonance assignments for the WT complexes were derived using a series of TROSY-based 2D and 3D experiments recorded at a ^{1}H field of 600 or 800 MHz following a multi-pronged approach described previously for a similar system(5), including HNCO, HNCA, and HN(CA)CB triple-resonance experiments and SOFAST-based Hn-NHn NOESY experiments recorded at 800 MHz(6–10). Assignments were then transferred to the spectra of the open complexes and confirmed by TROSY-readout triple-resonance experiments (HNCO, HNCA, and HN(CA)CB), recorded at 600 MHz. Final backbone assignments were verified using the TALOS-N server (11) and deposited in the Biological Magnetic Resonance Bank (IDs: 51101 and 51781). For chemical shift perturbation calculations, the WT and open TROSY NMR spectra were aligned to each other using a residue far from the mutation sites as a reference

based on an existing crystal structure, in a region where open and WT peaks were perfectly overlapped (HLA-A*02:01_E254 and β_2m_D96; PDB ID: 3mrq). Amide backbone chemical shift perturbations between the WT and the open variant were calculated using the following equation, given the aligned ^{15}N and ^{1}H chemical shifts: $\Delta\delta(ppm) = \sqrt{(\Delta\delta_H)^2 + \left(\frac{\Delta\delta_N}{10}\right)^2}$. All NMR data were processed with NMRPipe and analyzed using NMRFAM-SPARKY and POKY(12, 13).

Hydrogen/Deuterium exchange mass spectrometry. The open HLA-A*02:01/KILGFVFJV was dialyzed into equilibration buffer (150 mM NaCl, 20 mM sodium phosphate, pH 6.5 in H_2O) and diluted to a stock concentration of 30 μM and then either i) kept on ice without exposure to UV light or ii) UV-exposed for 45 min at 4°C. Samples were prepared and injected manually for several deuterium-exchange incubation periods. 5 μL open HLA-A*02:01/KILGFVFJV (30 μM) with or without UV-irradiation were diluted with 20 μL equilibration buffer (all H experiments, 0 s) or deuterium buffer (150 mM NaCl, 20 mM sodium phosphate pD 6.5 in D_2O) to 6 μM. The proteins were incubated with deuterium buffer for 20, 180, and 600 seconds at RT, and 15 minutes at 43°C for open HLA-A*02:01/KILGFVFJV or at 34°C for UV-irradiated open HLA-A*02:01/KILGFVFJV as all the D samples for $\Delta Mass_{100\%}$. The samples were then quenched with an equal volume of acidic buffer (150 mM NaCl, 1 M TCEP, 20 mM sodium phosphate pH 2.35 in H_2O, 25 μL). Quenched proteins were immediately injected for LC-MS/MS, in which integrated pepsin digestion was performed using a C8 5 μM column and a Q Exactive Orbitrap Mass Spectrometer. Peptide fragments corresponding to HLA-A*02:01 and β_2m were identified using Thermo Proteome Discoverer v2.4. The percent deuterium uptake was back-exchange corrected for each time point using the following equation(14): $D=\frac{\Delta Mass_T - \Delta Mass_{0\%}}{\Delta Mass_{100\%} - \Delta Mass_{0\%}}$. ExMs2 program was used to identify and analyze deuterated peptides. Measured deuterium uptakes for peptide fragments at 600s were averaged to each amino acids based on the start and end position of the peptide. The kinetic plots and the scaled B factor for the structure plot were generated by python3 and PyMOL(15).

Fluorescence polarization. The kinetic association of fluorescently labeled peptides and various peptide-loaded MHC-I was monitored by fluorescence polarization (FP). An optimized concentration of a fluorophore-labeled peptide (determined via serial dilution that yields a polarization baseline between 0 and 50 mP) was solubilized in FP buffer (150 mM NaCl, 20 mM sodium phosphate, 0.05% Tween-20, pH 7.4). MHC-I proteins and fluorophore-labeled peptides were directly added to the plate to 100 μL per well to avoid extended incubation and loss of data. The kinetic association was monitored for 2-12 hours, and polarization measurements were recorded every 28-105 seconds. The WT or open pMHC-I concentration remained constant across experiments at 200 nM, except for the MHC titration assays. Excitation and emission values used to monitor the fluorescence of TAMRA-labeled peptides were 531 and 595 nm, and FITC-labeled peptides were 475 and 525 nm. All experiments were performed in triplicates at RT. For IC_{50} competition assays, a serial dilution of competitor peptide was added to 200 nM WT or open pMHC-I and

the optimal concentration of fluorophore-labeled peptide. Kinetic association measurements were collected. Non-linear regression fitting allowed calculating plateau polarization (mP) values for each kinetic curve. Log transformed values of each peptide concentration were plotted against the plateau mP value, and an IC_{50} curve was fit using log(inhibitor) vs. response (three parameters) curve from GraphPad Prism v9. Raw parallel ($I_{\parallel}$) and perpendicular emission intensities ($I_{\perp}$) were collected and converted to polarization (mP) values using the equation $1000*[(I_{\parallel}-(G*I_{\perp}))/(I_{\parallel}+(G*I_{\perp}))]$. An optimized G-factor was determined to be 0.33 for TAMRA-labeled peptides and 0.4 for FITC-labeled peptides in calculating baseline fluorescence and overall FP. The data analysis method was adapted and data was fitted in GraphPad Prism v9(16).

Biotinylation and tetramer formation. Biotinylation and tetramer formation of the WT and open HLA-A*02:01/KILGFVFβFV proteins were performed as previously described(17). The BSP-tagged proteins were biotinylated using the BirA biotin-protein ligase bulk reaction kit (Avidity) according to the manufacturer's instructions and prepared at a final concentration of 2 mg/mL monomer. The level of biotinylation was evaluated by SDS-PAGE gel shift assay in the presence of excess streptavidin. Biotinylated WT and open HLA-A*02:01/KILGFVFβFV were then mixed with 10-fold molar excess of the NYESO-1 peptide variants, SLLMWITQV, SLLMWITQC, and SLLMWITQA. Each reaction was incubated 2 hours at room temperature and the peptide exchange reactions were confirmed by DSF. Meanwhile, streptavidin-PE (Agilent Technologies, Inc.) at 4:1 monomer/streptavidin molar ratio was added to HLA-A*02:01/KILGFVFβFV in the presence of excess peptides over 10-time intervals every 10 mins at RT in the dark. Tetramerized molecules upon peptide exchange were washed using Amicon Ultra centrifugal filter units with a 100 kDa membrane cut-off. Biotinylated WT and open HLA-A*02:01/KILGFVFβFV proteins, which did not require peptide exchange, were prepared the same way as peptide exchanged molecules incubating the same amount of buffer. The resulting tetramers can be stored at 4°C for up to 4 weeks.

1G4 TCR lentivirus production. Lenti-X 293T cells (Takara) were cultured in DMEM (Gibco), 10% FBS (Gibco), and Glutamax (Gibco) and were plated one day before transfection. Cells were transfected at a confluency of 80-90% with TransIT-293 (Mirus) using pMD2.G (Addgene #12259, gift from Didier Trono), psPAX2 (Addgene #12260, gift from Didier Trono), and pSFFV-1G4. Virus-containing media was collected 24- and 48-hours post-transfection, clarified by centrifugation at 500 g for 10 min, and incubated with Lenti-X concentrator (Takara) for at least 24 hours. Virus was pooled and concentrated 50-100x, resuspended in PBS, aliquoted, and stored at -80°C for subsequent T cell infections.

Primary human T cell tetramer staining. Healthy donor T cells were processed by the Human Immunology Core at the University of Pennsylvania by magnetic separation of CD8+ T cells. Cells were cultured in Advanced RPMI (Gibco), 10% heat inactivated FBS (Gibco), Glutamax (Gibco), penicillin/streptomycin (Gibco), and 10mM HEPES (Quality Biological), supplemented with 300 U/mL recombinant IL-2 (NCI Biological Resources Branch). T cells were maintained at ~1 million cells/mL and

were activated with a 1:1 ratio of Dynabeads Human T-Activator CD3/CD28 beads (Gibco) for 48 hours. 24 hours after initial activation, cells were either left untransduced or transduced with lentivirus expressing the 1G4 TCR. Cells were debeaded by magnetic separation and expanded in the presence of IL-2. Transduction efficiency was determined by staining with an anti-Vβ13.1-APC antibody (Miltenyi Biotec.), typically greater than 50%. Cells were cryopreserved with CryoStor CS10 (StemCell Technologies). Thawed T cells were recovered and regrown in IL-2-containing complete media for ~3 days prior to staining. Cells were harvested and washed with PBS/1% BSA/2 mM EDTA with 5 µg/mL PE-conjugated tetramer and incubated for 25 min at room temperature with slight shaking. After two washes with an RPMI-based wash buffer containing 1% FBS, cells were resuspended in 1:1000 Sytox Blue diluted in wash buffer to distinguish dead cells. Samples were processed on an CytoFLEX LX and the data analyzed by FlowJo v10.8.1.

References

1. B. Reynisson, B. Alvarez, S. Paul, B. Peters, M. Nielsen, NetMHCpan-4.1 and NetMHCIIpan-4.0: improved predictions of MHC antigen presentation by concurrent motif deconvolution and integration of MS MHC eluted ligand data. *Nucleic Acids Research* **48**, W449 (2020).

2. H. Li, K. Natarajan, E. L. Malchiodi, D. H. Margulies, R. A. Mariuzza, Three-dimensional structure of H-2Dd complexed with an immunodominant peptide from human immunodeficiency virus envelope glycoprotein 12011Edited by I. A. Wilson. *Journal of Molecular Biology* **283**, 179–191 (1998).

3. A. C. McShan, *et al.*, Molecular determinants of chaperone interactions on MHC-I for folding and antigen repertoire selection. *Proc. Natl. Acad. Sci. U.S.A.* **116**, 25602–25613 (2019).

4. V. Tugarinov, V. Kanelis, L. E. Kay, Isotope labeling strategies for the study of high-molecular-weight proteins by solution NMR spectroscopy. *Nat Protoc* **1**, 749–754 (2006).

5. K. Natarajan, *et al.*, An allosteric site in the T-cell receptor Cβ domain plays a critical signalling role. *Nat Commun* **8**, 15260 (2017).

6. P. Rossi, Y. Xia, N. Khanra, G. Veglia, C. G. Kalodimos, 15N and 13C- SOFAST-HMQC editing enhances 3D-NOESY sensitivity in highly deuterated, selectively [1H,13C]-labeled proteins. *J Biomol NMR* **66**, 259–271 (2016).

7. D. Marion, L. E. Kay, S. W. Sparks, D. A. Torchia, A. Bax, Three-dimensional heteronuclear NMR of nitrogen-15 labeled proteins. *J. Am. Chem. Soc.* **111**, 1515–1517 (1989).

8. M. Salzmann, K. Pervushin, G. Wider, H. Senn, K. Wüthrich, TROSY in triple-resonance experiments: New perspectives for sequential NMR assignment of large proteins. *Proc Natl Acad Sci U S A* **95**, 13585–13590 (1998).

9. S. Grzesiek, A. Bax, Improved 3D triple-resonance NMR techniques applied to a 31 kDa protein. *Journal of Magnetic Resonance (1969)* **96**, 432–440 (1992).

10. L. E. Kay, M. Ikura, R. Tschudin, A. Bax, Three-dimensional triple-resonance NMR spectroscopy of isotopically enriched proteins. *Journal of Magnetic Resonance (1969)* **89**, 496–514 (1990).

11. Y. Shen, A. Bax, Protein backbone and sidechain torsion angles predicted from NMR chemical shifts using artificial neural networks. *J Biomol NMR* **56**, 227–241 (2013).

12. F. Delaglio, *et al.*, NMRPipe: a multidimensional spectral processing system based on UNIX pipes. *J Biomol NMR* **6**, 277–293 (1995).

13. W. Lee, *et al.*, Backbone resonance assignments and secondary structure of Ebola nucleoprotein 600-739 construct. *Biomol NMR Assign* **13**, 315–319 (2019).

14. G. R. Masson, *et al.*, Recommendations for performing, interpreting and reporting hydrogen deuterium exchange mass spectrometry (HDX-MS) experiments. *Nat Methods* **16**, 595–602 (2019).

15. Schrödinger, LLC, The PyMOL Molecular Graphics System, Version 1.8 (2015).

16. R. Buchli, *et al.*, Real-Time Measurement of in Vitro Peptide Binding to Soluble HLA-A*0201 by Fluorescence Polarization. *Biochemistry* **43**, 14852–14863 (2004).

17. S. A. Overall, *et al.*, High throughput pMHC-I tetramer library production using chaperone-mediated peptide exchange. *Nature Communications* **11**, 1909 (2020).

18. X. Robert, P. Gouet, Deciphering key features in protein structures with the new ENDscript server. *Nucleic Acids Res* **42**, W320–W324 (2014).

19. M. C. F. Thomsen, M. Nielsen, Seq2Logo: a method for construction and visualization of amino acid binding motifs and sequence profiles including sequence weighting, pseudo counts and two-sided representation of amino acid enrichment and depletion. *Nucleic Acids Research* **40**, W281–W287 (2012).

20. D. J. Barker, *et al.*, The IPD-IMGT/HLA Database. *Nucleic Acids Res*, gkac1011 (2022).

21. F. Sievers, *et al.*, Fast, scalable generation of high-quality protein multiple sequence alignments using Clustal Omega. *Mol Syst Biol* **7**, 539 (2011).

Supplemental Figures

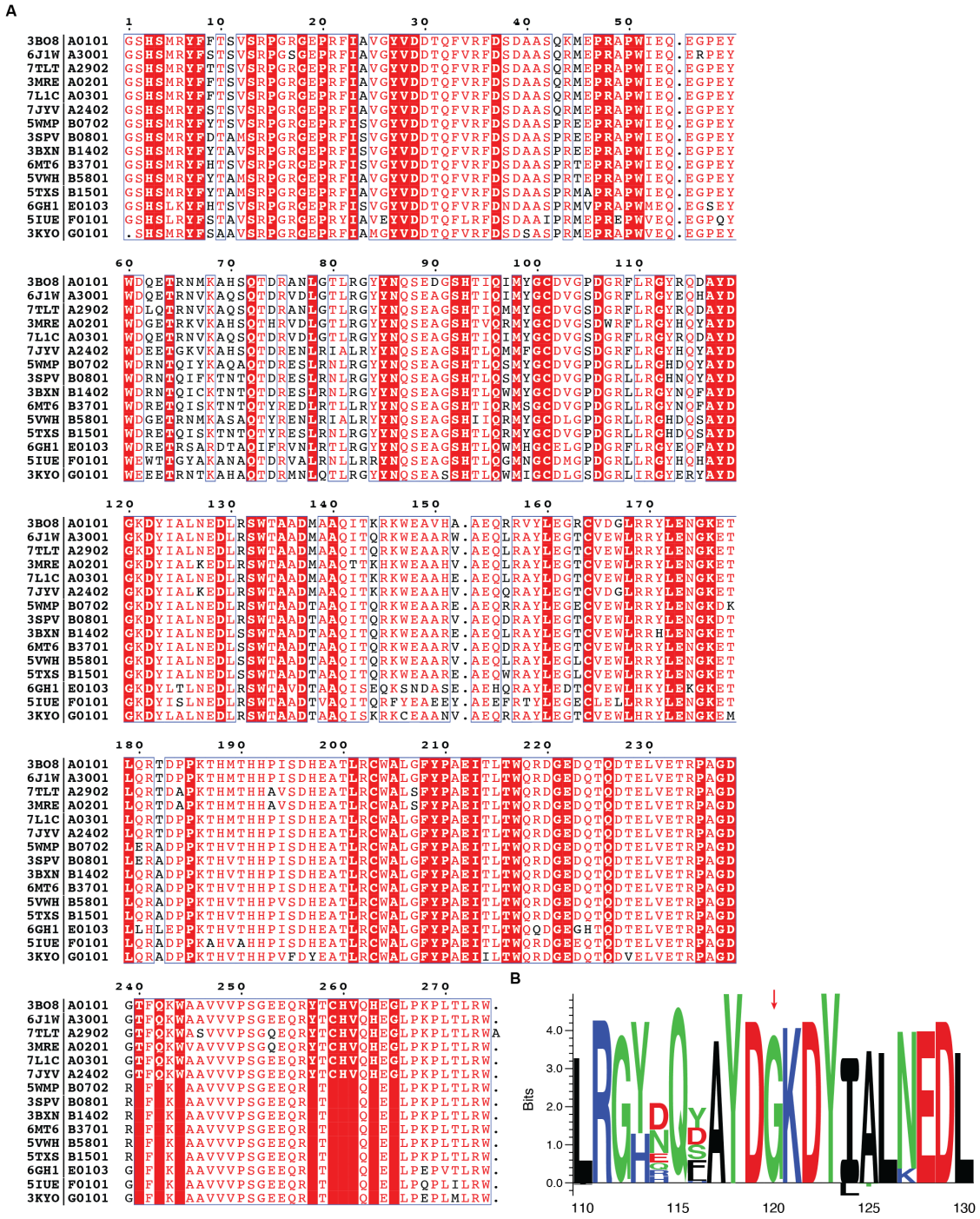

Figure S1. Sequence alignment of distinct HLA allotypes across HLA-A, B, and C as well as HLA-Ib. **A.** Sequence alignment of the HLA representatives were extracted from the Protein data bank and processed using ESPript(18), covering HLA-A and HLA-B supertypes as well as HLA-Ib, PDB ID as indicated. **B.** Seq2logo visualization(19) of the sequence alignment for 75 distinct HLA allotypes with >1% global population frequency shows a conserved residue G120. Sequence weighting used clustering,

pseudo count with a weight of 0, and Kullback–Leibler logotype. The percentage frequency of amino acids on a specific position higher than 10% is shown on the positive *y*-axis, and less than 10% amino acids on the negative y-axis. Allele sequences were derived from the IPD-IMGT/HLA(20) and the alignment was performed using ClustalOmega(21).

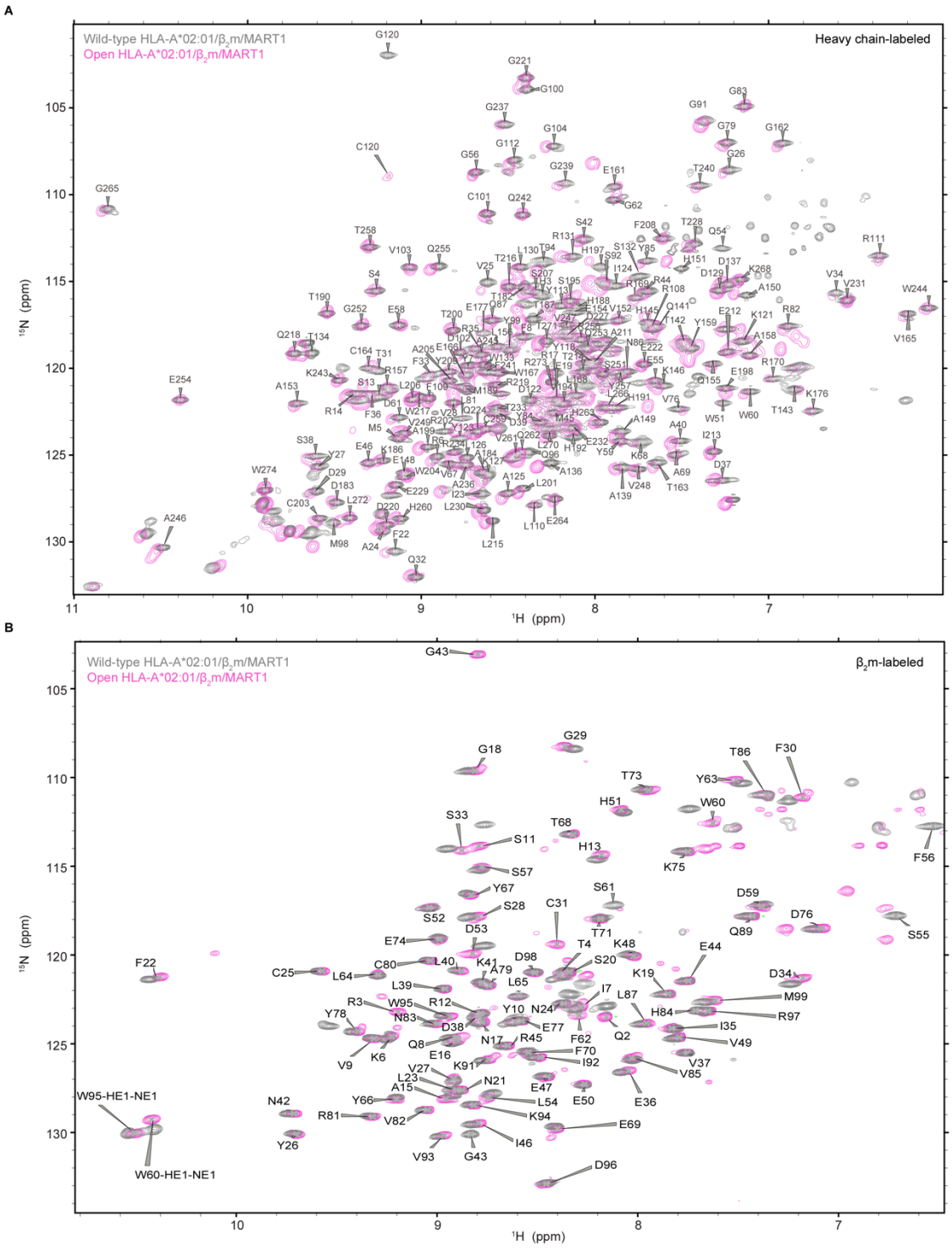

Figure S2. Overlay of the WT and open MHC-I NMR spectra reveal substantial backbone chemical shift changes. 2D ^{1}H-^{15}N TROSY spectra of [^{1}H, ^{13}C, ^{15}N]-labeled **A.** HC (HLA-A*02:01) refolded with unlabeled light chain (β2m) and MART1 (ELAGIGILTV), or **B.** β2m bound to unlabeled HC and MART1. Spectra represent the WT complex collected at 800 MHz ^{1}H magnetic field (in gray), overlayed by the open

253 complex spectra collected at 600 MHz ^{1}H magnetic field (in pink). All data were collected with identical
254 buffer conditions (20 mM sodium phosphate, pH 7.2, and 150 mM NaCl) and at RT (298-300 K).

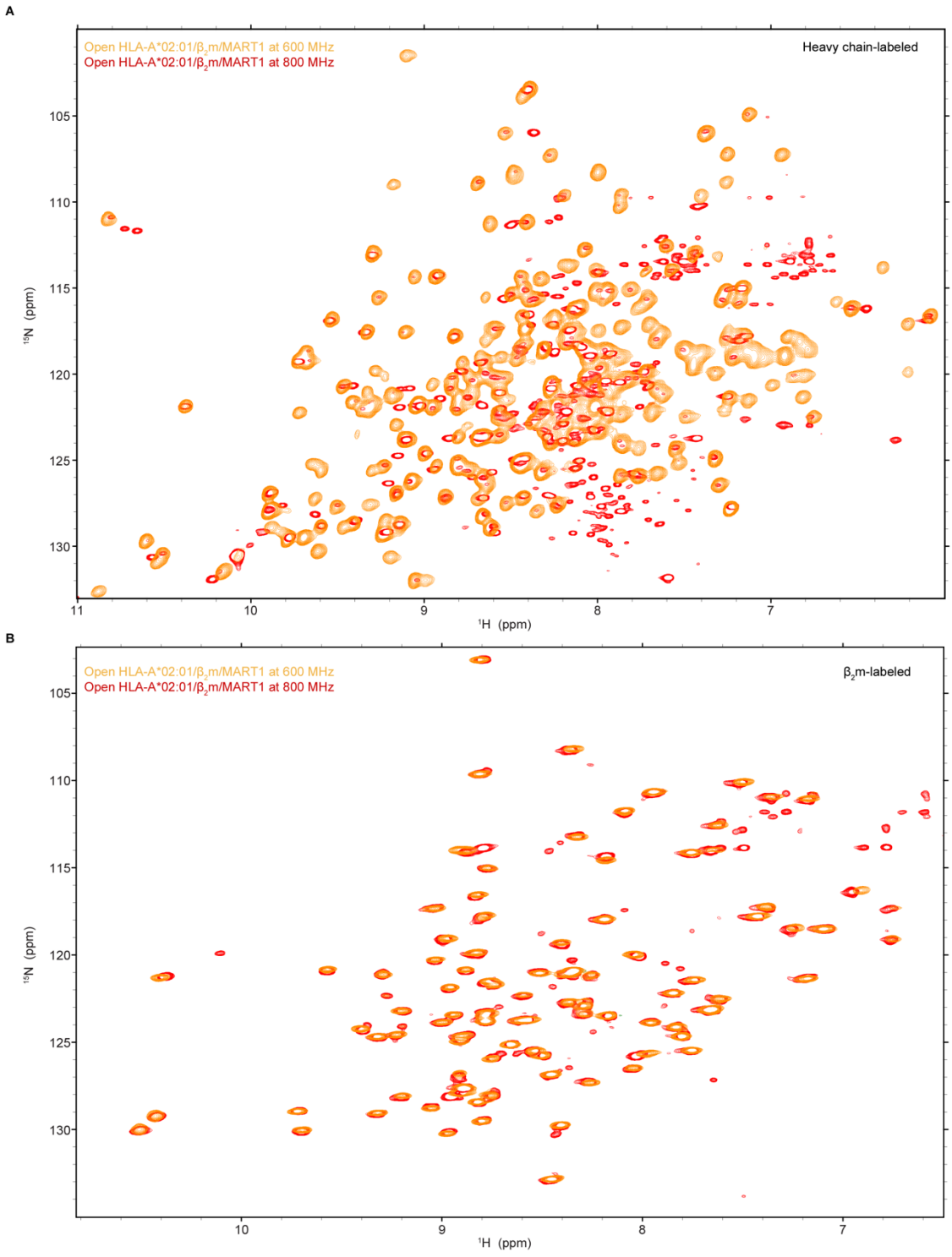

Figure S3. Overlay of NMR spectra for the open MHC-I confirms the same backbone chemical shifts regardless of the magnetic field. ^{1}H-^{15}N TROSY data collected for the open HLA-A*02:01/β_2m/ MART1 at both 600 MHz (orange) and 800 MHz (red) for [^{1}H, ^{13}C, ^{15}N]-labeled HC refolded with β_2m and MART1 (top), or β_2m bound to unlabeled HC and MART1 (bottom). Additional peaks in the spectra collected at 800 MHz are largely due to protein degradation and do not affect the chemical shifts corresponding to the protein

backbone. All data were collected with identical buffer conditions (20 mM sodium phosphate, pH 7.2, and 150 mM NaCl) and at RT (298-300 K).

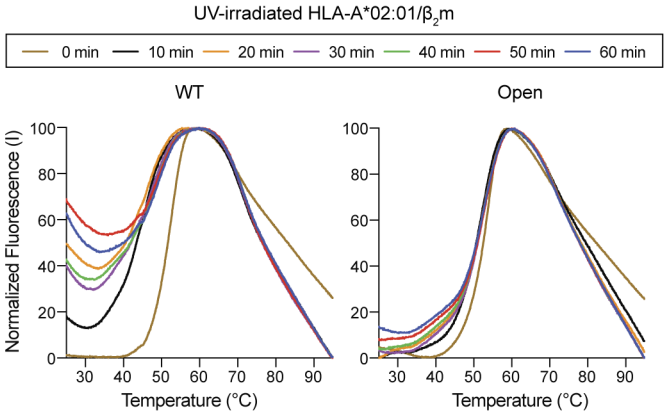

Figure S4. Differential Scanning Fluorimetry curves of UV-irradiated WT or open HLA-A*02:01/β_2m. Thermal stability curves were obtained using DSF for the WT (left) and open (right) HLA-A*02:01/β_2m with a photocleavable peptide KILGFVFJV upon UV irradiation without the presence of a rescuing peptide. The duration of UV exposure was indicated by different colors from 0 to 60 mins with intervals of 10 mins. Normalized fluorescence (I) at 25°C was extracted and plotted against the duration of UV exposure in **Fig. 3A**. Results of three technical replicates (mean ± σ) are plotted.

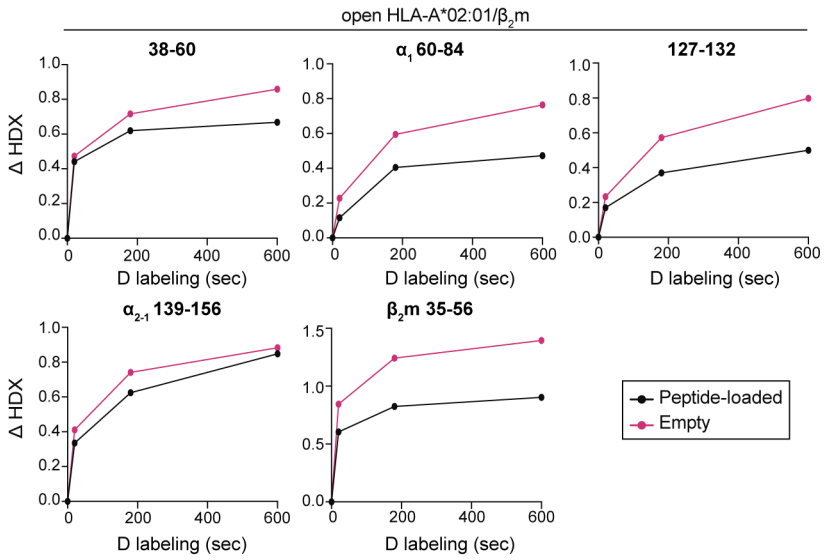

Figure S5. Deuterium uptake resolved to individual peptide fragments for open HLA-A*02:01/β_2m. Peptide segments of 38-60, α_1 60-84, 127-132, $\alpha_{2\text{-}1}$ 139-156, and β_2m 35-56 are plotted for each exposure time (0, 20, 180, and 600s). The plots reveal the local HDX profiles of open HLA-A*02:01 for the states of peptide-loaded (black, refolded with KILGFVFJV) and empty (pink, 40-minute UV irradiation at 4°C).

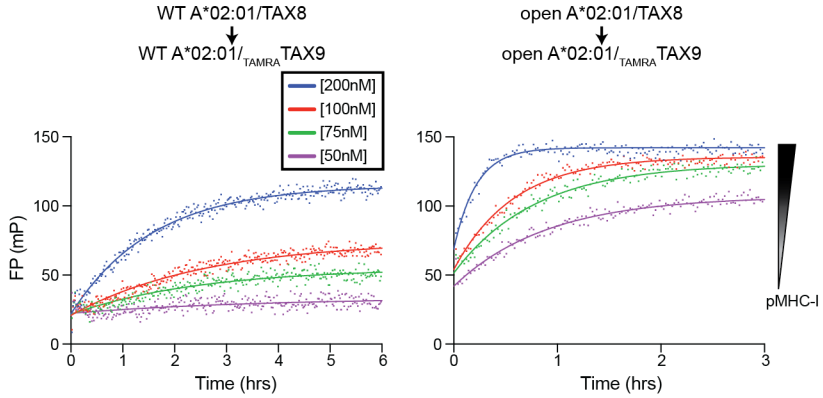

275

276 **Figure S6. Binding of $_{TAMRA}$TAX9 by the WT or open HLA-A*02:01/TAX8.** Peptide exchange measured
277 by fluorescence polarization (mP) of 40nM $_{TAMRA}$TAX9 as a function of the WT or open HLA-A*02:01/TAX8
278 concentrations. Individual traces were fit to a monoexponential association model to determine apparent
279 rate constants $K_{assoc.}$ plotted in **Fig. 4D**. Results of three replicates (mean) are plotted.

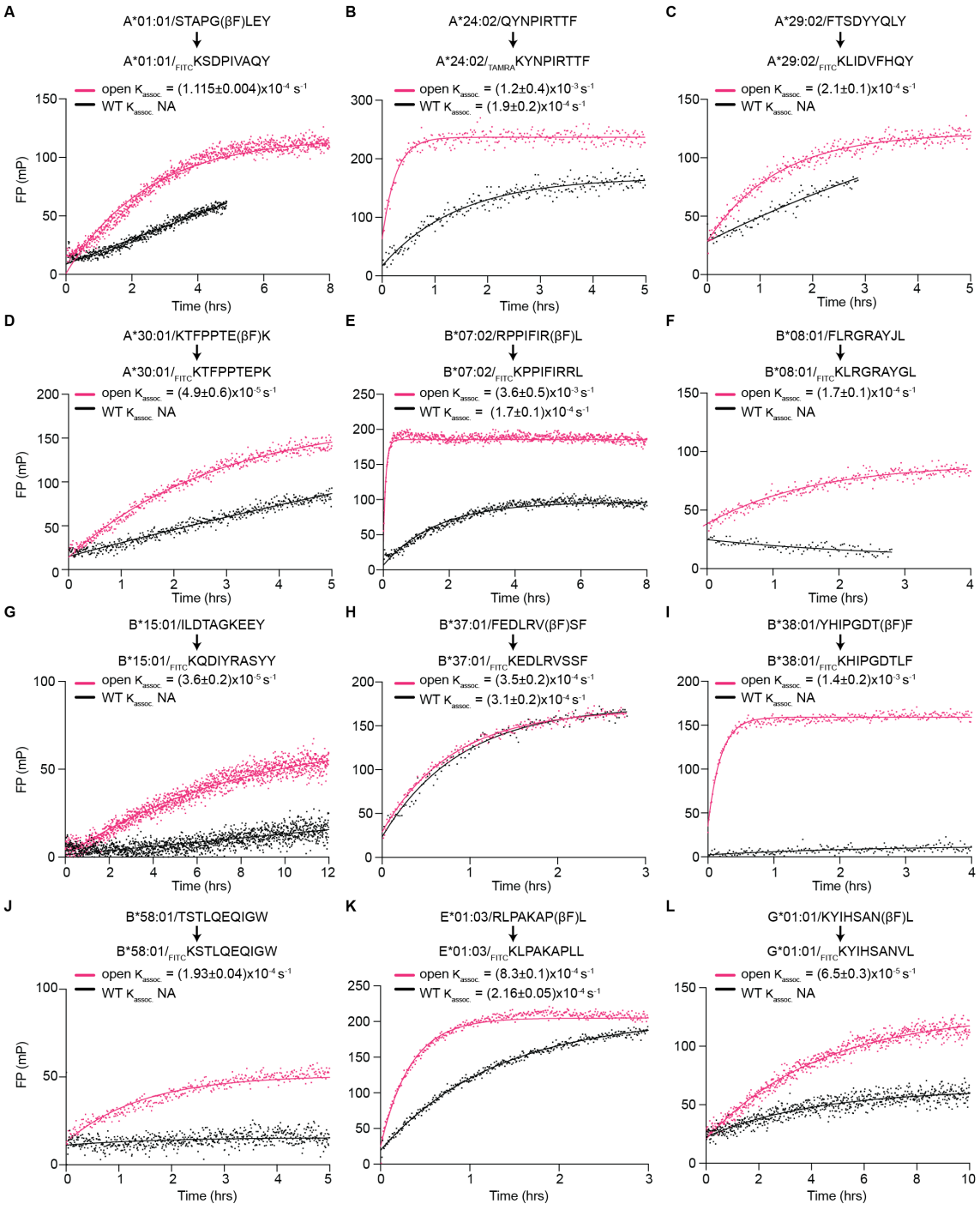

Figure S7. Peptide exchange kinetics of the open vs. WT HLA allotypes. A-L, The association profiles of fluorophore-conjugated peptides $_{FITC}$KSDPIVAQY, $_{TAMRA}$KYNPIRTTF, $_{FITC}$KLIDVFHQY, $_{FITC}$KTFPPTEPK, $_{FITC}$KPPIFIRRL, $_{FITC}$KLRGRAYGL, $_{FITC}$KQDIYRASYY, $_{FITC}$KEDLRVSSF, $_{FITC}$KHIPGDTLF, $_{FITC}$KSTLQEQIGW, $_{FITC}$KLPAKAPLL, and $_{FITC}$KYIHSANVL to the open (pink) and WT (black) HLA- **A.** A*01:01/STAPG(βF)LEY, **B.** A*24:02/QYNPIRTTF, **C.** A*29:02/FTSDYYQLY, **D.** A*30:01/KTFPPTE(βF)K, **E.** B*07:02/RPPIFIR(βF)L, **F.** B*08:01/FLRGRAYJL, **G.** B*15:01/ILDTAGKEEY, **H.**

B*37:01/FEDLRV(βF)SF, **I.** B*38:01/YHIPGDT(βF)F, **J.** B*58:01/TSTLQEQIGW, **K.** E*01:03/RLPAKAP(βF)L, and **L.** G*01:01/KYIHSAN(βF)L. The data were fitted to a monoexponential association model to determine apparent rate constants $K_{assoc.}$ NA means the $K_{assoc.}$ cannot be fitted. Results of three replicates (mean ± σ) are plotted**.**

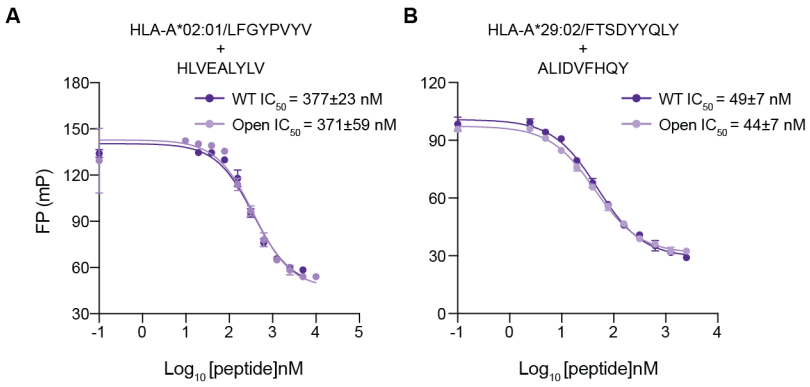

291

292 **Figure S8. Selected T1D epitopes demonstrate the same IC50 profiles for the WT or open MHC-I.**
293 The IC_{50} profiles extracted from the association profiles of **A.** $_{TAMRA}$KLFGYPVYV binding to HLA-
294 A*02:01/TAX8 and **B.** $_{FITC}$KLIDVFHQY binding to HLA-A*29:02/FTSDYYQLY in a concentration gradient of
295 a competitor HLVEALYLV and ALIDVFHQY peptides, respectively. IC_{50} values were determined by fitting
296 a log(inhibitor) vs. response (three parameters) curve. Results of three replicates (mean ± σ) are plotted.

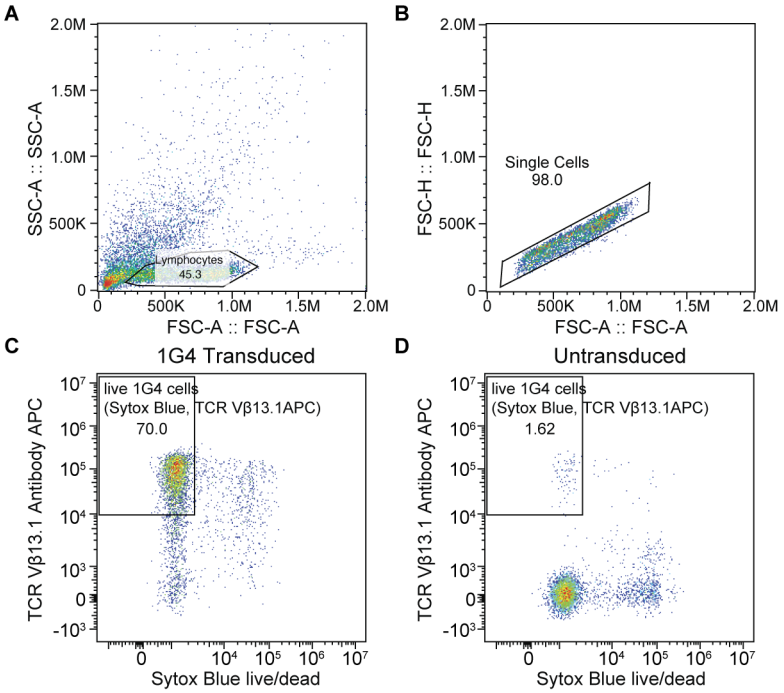

Figure S9. Flow cytometry gating strategy of CD8+ T cells transduced with 1G4. A-B. Previously transduced or non-transduced primary human CD8+ T cells were thawed and recovered before tetramer staining. Cells were sorted by side and forward scatter (**A.** SSC-A and FSC-A) followed by single cell isolation (**B.** FSC-A versus FSC-H plot). **C-D.** Gating for live cells was determined by Sytox blue staining, and transduction efficiency was determined by staining with an anti-Vβ13.1-APC antibody (Miltenyi Biotec). Gates are shown in black, and the percentages of events are gated in parentheses. The acquisition was performed on CytoFLEX LX (Beckman Coulter), and the data were analyzed by FlowJo v10.8.1.

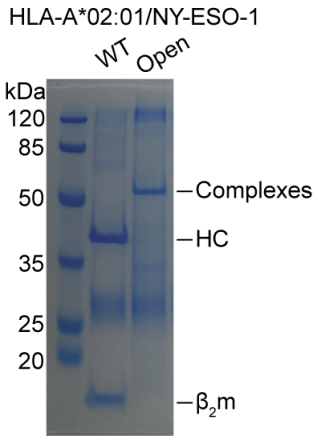

Figure S10. Refolded WT HLA-A*02:01/NY-ESO-1 upon tetramerization maintain β_2m. 2 μg of WT and open HLA-A*02:01/NY-ESO-1 in tetrameric form conjugated with fluorophore PE was loaded and ran on an SDS/PAGE gel, confirming the existence of β_2m upon vigorous wash during tetramerization.

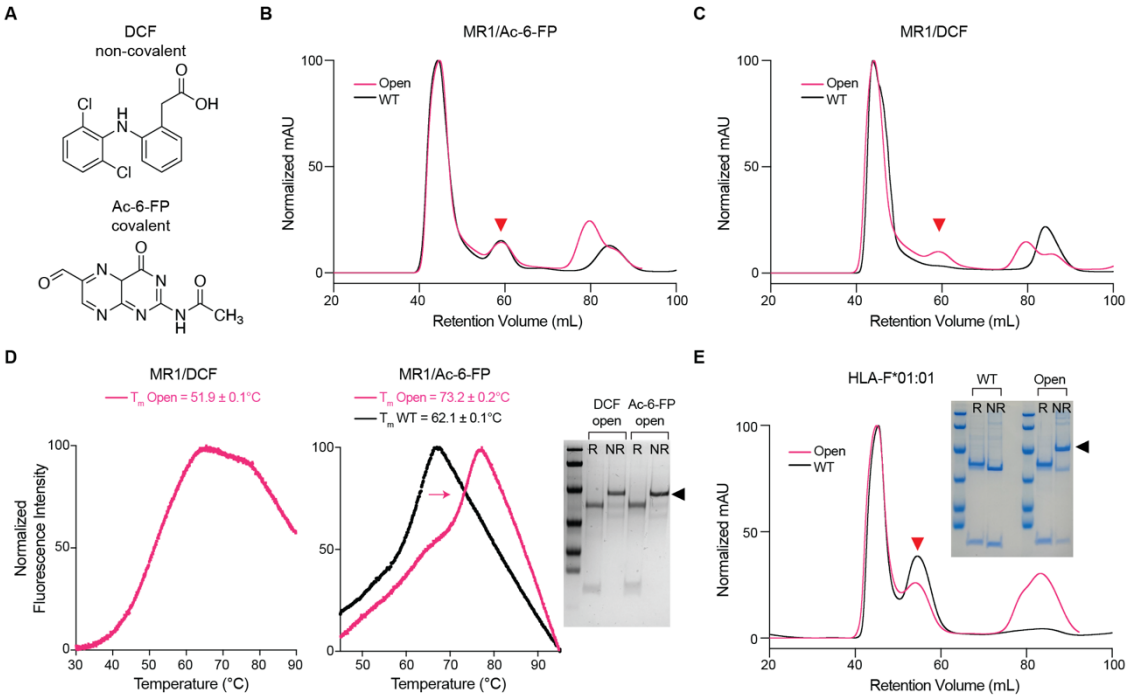

Figure S11. Disulfide-engineered open MR1 and HLA-F*01:01 molecules form stable protein complexes. A. Chemical structures of MR1 ligands DCF and Ac-6-FP. **B-C.** SEC traces of the WT (black) and open (pink) MR1 C262S refolded with **B.** Ac-6-FP and **C.** DCF. The triangle arrowhead indicates the protein complexes. **D.** Melting temperature (T_m, ºC) obtained from DSF of the WT (black) and open (pink) MR1 C262S loaded with DCF or Ac-6-FP, which are further confirmed by SDS/PAGE analysis in reduced (R) or non-reduced (NR) conditions. Results of three technical replicates (mean ± σ) are plotted. **E.** SEC traces of the WT (black) and open (pink) HLA-F*01:01/β_2m. The triangle arrowheads indicate the complex peaks, further confirmed by SDS/PAGE analysis in reduced (R) or non-reduced (NR) conditions.

Supplemental Tables

#Peptide	Peptide sequence	Wild type		Open	
		T_m (°C)	σ (±°C)	T_m (°C)	σ (±°C)
1	KLVVVGACGV	48.81	0.11	52.19	0.09
2	LLGRNSFEVHV	43.42	0.38	48.66	0.21
3	KLVVVGAAGV	48.06	0.11	51.65	0.12
4	RLIRVEGNLRV	53.37	0.25	53.33	0.17
5	KLVVVGASGV	46.22	0.05	49.86	0.12
6	ALNNMFCQLA	44.42	0.11	51.07	0.40
7	ILNREIDFA	48.69	0.07	53.00	0.18
8	KTYPVQLWV	49.35	0.11	54.49	0.35
9	GLAPPQHRI	44.05	0.15	49.20	0.32
10	YMFNSSCMGGM	48.02	0.09	53.38	0.19
11	LLGRNSFEMRV	46.24	0.07	50.78	0.13
12	GLAPPQRLIRV	50.73	0.11	53.77	0.16
13	YLSTDVGFCT	48.30	0.11	53.88	0.19
14	VLMGHVAAVG	58.50	0.77	57.73	0.05
15	YLDSGIHFG	49.90	0.13	52.78	0.47
16	KILNREIDFAI	46.89	0.13	52.79	0.10
17	YMCNSSCMGV	60.98	3.22	58.62	0.21
18	YSSGFCNIAV	43.73	0.06	49.31	0.16
19	LLVRNSFEV	53.93	0.29	57.38	0.11
20	ILWRQDIHLGV	53.91	0.08	57.55	0.04
21	MFCQLAKTYPV	43.67	0.23	54.24	0.36
22	LLVRNSFEVRV	44.32	0.06	51.30	0.22
23	IDILWRQDIHL	44.83	0.06	51.71	0.61
24	KLVVVGADGV	45.08	0.11	49.77	0.09
25	GMNWRPILTI	42.32	0.33	50.04	0.07
26	ILCATYVKV	57.41	0.36	59.44	0.12
27	LLGRNSFEVLV	42.80	0.24	48.85	0.20
28	LLDILDTAGL	40.96	0.05	49.75	0.09
29	CLLDILDTAGL	46.69	0.04	54.21	0.22
30	FSGEYIPTV	56.01	0.51	58.30	0.05
31	RPLAWGNINL	44.02	0.12	48.17	0.22
32	ILNREIDFAI	44.95	0.08	52.01	0.14
33	GLKDLLNPI	53.70	0.24	54.58	0.29

34	YLDSGIHCGA	51.99	0.38	54.34	0.20
35	FCQLAKTYPV	50.19	0.27	52.29	0.10
36	ILWRQDIHL	55.74	0.37	58.83	0.02
37	GLVDEQQEV	54.49	0.30	54.61	0.26
38	NLLVRNSFEV	47.57	0.22	49.85	0.20
39	KLVVVGAVGV	49.24	0.17	52.59	0.12
40	KILCATYVKV	47.90	0.44	51.72	0.09
41	YLSTDVGFCTL	50.29	0.25	54.63	0.10
42	FMKQMNDAL	43.99	0.50	49.62	0.04
43	YLDSGIHFGA	54.43	0.18	56.41	0.15
44	GLAPPQHLTRV	55.33	0.93	57.39	0.07
45	ALNNMFCQL	51.43	0.78	54.62	0.51
46	LLGRNSFEM	47.91	0.29	51.31	0.07
47	GLKDLLNPIGV	48.99	0.29	52.79	0.28
48	CQLAKTYPV	55.84	1.18	62.52	0.08
49	VLHECNSSYI	46.60	0.20	53.12	0.19
50	KLVVVGAGCV	47.64	0.13	49.39	0.09
TAX9	LLFGYPVYV	65.06	0.18	63.74	0.10
P29	YPNVNIHNF	41.99	0.15	48.72	0.07
TAX9 Refolded	LLFGYPVYV	64.20	0.19	64.44	0.06

Table S1. Thermal stabilities for Cancer Genome Atlas (TCGA) epitope library determined by DSF. T_m of individual peptides from the TCGA epitope library loaded on WT or open HLA-A*02:01 were measured via peptide exchange in triplicates. The high-affinity HLA-A*02:01-restricted TAX9 peptide and refolded TAX9/A02 molecules were used as positive controls, and the irrelevant peptide p29 was used as a negative control.

HLA Supertype	HLA Allele	Placeholder Ligand	Ligand Sequence	Melting Temperature			
				wild-type		open	
				T_m (°C)	σ (±°C)	T_m (°C)	σ (±°C)
A01	A*01:01	β-A01	STAPG(βF)LEY	43.75	0.02	61.2	0.5
A0103	A*30:01	β-A30	KTFPPTE(βF)K	49.18	0.08	51.05	0.09
A0124	A*29:02	SARS P44	FTSDYYQLY	53.97	0.07	53.46	0.08
A02	A*02:01	TAX8	LFGYPVYV	41.6	0.2	48.79	0.07
		TAX9	LLFGYPVYV	52.36	0.09	52.98	0.09
A24	A*24:02	Phox2B	QYNPIRTTF	66.0	0.1	63.23	0.05
B07	B*07:02	β-B07	RPPIFIR(βF)L	44.8	0.1	48.5	0.3
B08	B*08:01	PhotoB08	FLRGRAYJL	56.5	0.2	55.93	0.07
B27	B*38:01	β-B38	YHIPGDT(βF)F	49.4	0.2	50.7	0.1
B44	B*37:01	β-B37	FEDLRV(βF)SF	49.0	0.5	47.8	0.5
B58	B*58:01	TW10	TSTLQEQIGW	49.3	0.2	53.1	0.4
B62	B*15:01	nRASQ61K	ILDTAGKEEY	46.8	0.1	52.5	0.1
E	E*01:03	β-E01	RLPAKAP(βF)L	49.2	0.1	51.1	0.1
G	G*01:01	β-G01	KYIHSAN(βF)L	60.4	0.1	51.0	0.2
MR1	MR1 C262S	Diclofenac	-	-	-	51.9	0.1
		Ac-6-FP	-	62.1	0.1	73.2	0.2

Table S2. Summary of the designed placeholder peptides and the T_m. Melting temperatures (T_m) were determined for the WT and mutant HLA allotype representatives. Each allotype was refolded with a selected placeholder peptide and its T_m was determined by three technical replicates.

Classical HLA Alleles	
HLA-A Supertypes	
Allele	Protein Sequence
A*02:01	M**G**SHSMRYFFTSVSRPGRGEPRFIAVGYVDDTQFVRFDSDAASQRMEPRAPWIEQEGP EYWDGETRKVKAHSQTHRVDLGTLRGYYNQSEAGSHTVQRMYGCDVGSDWRFLRGYH QYAYD**C**KDYIALKEDLRSWTAADMAAQTTKHKWEAAHVAEQLRAYLEGTCVEWLRRYLE NGKETLQRTDAPKTHMTHHAVSDHEATLRCWALSFYPAEITLTWQRDGEDQTQDTELVE TRPAGDGTFQKWAAVVVPSGQEQRYTCHVQHEGLPKPLTLRWEPGSLHHILDAQKMVW NHR
A*01:01	MAS**G**SHSMRYFFTSVSRPGRGEPRFIAVGYVDDTQFVRFDSDAASQKMEPRAPWIEQE GPEYWDQETRNMKAHSQTDRANLGTLRGYYNQSEDGSHTIQIMYGCDVGPDGRFLRGY RQDAYD**C**KDYIALNEDLRSWTAADMAAQITKRKWEAVHAAEQRRVYLEGRCVDGLRRYL ENGKETLQRTDPPKTHMTHHPISDHEATLRCWALGFYPAEITLTWQRDGEDQTQDTELV ETRPAGDGTFQKWAAVVVPSGEEQRYTCHVQHEGLPKPLTLRWELSSQPGSLHHILDAQ KMVWNHR
A*24:02	MAS**G**SHSMRYFSTSVSRPGRGEPRFIAVGYVDDTQFVRFDSDAASQRMEPRAPWIEQE GPEYWDEETGKVKAHSQTDRENLRIALRYYNQSEAGSHTLQMMFGCDVGSDGRFLRGY HQYAYD**C**KDYIALKEDLRSWTAADMAAQITKRKWEAAHVAEQQRAYLEGTCVDGLRRYL ENGKETLQRTDPPKTHMTHHPISDHEATLRCWALGFYPAEITLTWQRDGEDQTQDTELV ETRPAGDGTFQKWAAVVVPSGEEQRYTCHVQHEGLPKPLTLRWEPSSQPGSLHHILDA QKMVWNHR
A*29:02	M**G**SHSMRYFTTSVSRPGRGEPRFIAVGYVDDTQFVRFDSDAASQRMEPRAPWIEQEGP EYWDLQTRNVKAQSQTDRANLGTLRGYYNQSEAGSHTIQMMYGCDVGSDGRFLRGYR QDAYD**C**KDYIALNEDLRSWTAADMAAQITQRKWEAARVAEQLRAYLEGTCVEWLRRYLE NGKETLQRTDAPKTHMTHHAVSDHEATLRCWALSFYPAEITLTWQRDGEDQTQDTELVE TRPAGDGTFQKWASVVVPSGQEQRYTCHVQHEGLPKPLTLRWEPGSLHHILDAQKMVW NHR
A*30:01	M**G**SHSMRYFSTSVSRPGSGEPRFIAVGYVDDTQFVRFDSDAASQRMEPRAPWIEQERP EYWDQETRNVKAQSQTDRVDLGTLRGYYNQSEAGSHTIQIMYGCDVGSDGRFLRGYEQ HAYD**C**KDYIALNEDLRSWTAADMAAQITQRKWEAARWAEQLRAYLEGTCVEWLRRYLEN GKETLQRTDPPKTHMTHHPISDHEATLRCWALGFYPAEITLTWQRDGEDQTQDTELVET RPAGDGTFQKWAAVVVPSGEEQRYTCHVQHEGLPKPLTLRWELGSLHHILDAQKMVWN HR
HLA-B Supertypes	
Allele	Protein Sequence

B*07:02	MGSHSMRYFYTSVSRPGRGEPRFISVGYVDDTQFVRFDSDAASPREEPRAPWIEQEGPE YWDRNTQIYKAQAQTDRESLRNLRGYYNQSEAGSHTLQSMYGCDVGPDGRLLRGHDQY AYDCKDYIALNEDLRSWTAADTAAQITQRKWEAAREAEQRRAYLEGECVEWLRRYLENG KDKLERADPPKTHVTHHPISDHEATLRCWALGFYPAEITLTWQRDGEDQTQDTELVETRP AGDRTFQKWAAVVVPSGEEQRYTCHVQHEGLPKPLTLRWEPSSQSGSLHHILDAQKMV WNHR
B*08:01	MASGSHSMRYFDTAMSRPGRGEPRFISVGYVDDTQFVRFDSDAASPREEPRAPWIEQE GPEYWDRNTQIFKTNTQTDRESLRNLRGYYNQSEAGSHTLQSMYGCDVGPDGRLLRGH NQYAYDCKDYIALNEDLRSWTAADTAAQITQRKWEAARVAEQDRAYLEGTCVEWLRRYL ENGKDTLERADPPKTHVTHHPISDHEATLRCWALGFYPAEITLTWQRDGEDQTQDTELVE TRPAGDRTFQKWAAVVVPSGEEQRYTCHVQHEGLPKPLTLRWEPSSQSGSLHHILDAQK MVWNHR
B*15:01	MGSHSMRYFYTAMSRPGRGEPRFIAVGYVDDTQFVRFDSDAASPRMAPRAPWIEQEGP EYWDRETQISKTNTQTYRESLRNLRGYYNQSEAGSHTLQRMYGCDVGPDGRLLRGHDQ SAYDCKDYIALNEDLSSWTAADTAAQITQRKWEAAREAEQWRAYLEGLCVEWLRRYLEN GKETLQRADPPKTHVTHHPISDHEATLRCWALGFYPAEITLTWQRDGEDQTQDTELVETR PAGDRTFQKWAAVVVPSGEEQRYTCHVQHEGLPKPLTLRWEPSSQSGSLHHILDAQKM VWNHR
B*37:01	MGSHSMRYFHTSVSRPGRGEPRFISVGYVDDTQFVRFDSDAASPRTEPRAPWIEQEGPE YWDRETQISKTNTQTYREDLRTLLRYYNQSEAGSHTIQRMSGCDVGPDGRLLRGYNQFA YDCKDYIALNEDLSSWTAADTAAQITQRKWEAARVAEQDRAYLEGTCVEWLRRYLENGK ETLQRADPPKTHVTHHPISDHEATLRCWALGFYPAEITLTWQRDGEDQTQDTELVETRPA GDRTFQKWAAVVVPSGEEQRYTCHVQHEGLPKPLTLRWEPGSLHHILDAQKMVWNHR
B*38:01	MGSHSMRYFYTSVSRPGRGEPRFISVGYVDDTQFVRFDSDAASPREEPRAPWIEQEGPE YWDRNTQISKTNTQTYRENLRIALRYYNQSEAGSHTLQRMYGCDVGPDGRLLRGHNQFA YDCKDYIALNEDLSSWTAADTAAQITQRKWEAARVAEQLRTYLEGTCVEWLRRYLENGK ETLQRADPPKTHVTHHPISDHEATLRCWALGFYPAEITLTWQRDGEDQTQDTELVETRPA GDRTFQKWAAVVVPSGEEQRYTCHVQHEGLPKPLTLRWEPGSLHHILDAQKMVWNHR
B*58:01	MGSHSMRYFYTAMSRPGRGEPRFIAVGYVDDTQFVRFDSDAASPRTEPRAPWIEQEGP EYWDGETRNMKASAQTYRENLRIALRYYNQSEAGSHIIQRMYGCDLGPDGRLLRGHDQS AYDCKDYIALNEDLSSWTAADTAAQITQRKWEAARVAEQLRAYLEGLCVEWLRRYLENG KETLQRADPPKTHVTHHPVSDHEATLRCWALGFYPAEITLTWQRDGEDQTQDTELVETR PAGDRTFQKWAAVVVPSGEEQRYTCHVQHEGLPKPLTLRWEPGSLHHILDAQKMVWNH R
HLA-Ib & Nonclassical Alleles	
Allele	Protein Sequence

E*01:03	M**G**SHSLKYFHTSVSRPGRGEPRFISVGYVDDTQFVRFDNDAASPRMVPRAPWMEQEGS EYWDRETRSARDTAQIFRVNLRTLRGYYNQSEAGSHTLQWMHGCELGPDGRFLRGYEQ FAYD**C**KDYLTLNEDLRSWTAVDTAAQISEQKSNDASEAEHQRAYLEDTCVEWLHKYLEK GKETLLHLEPPKTHVTHHPISDHEATLRCWALGFYPAEITLTWQQDGEGHTQDTELVETR PAGDGTFQKWAAVVVPSGEEQRYTCHVQHEGLPEPVTLRWEPGSGGGLNDIFEAQKIE WHE
G*01:01	M**G**SHSMRYFSAAVSRPGRGEPRFIAMGYVDDTQFVRFDSDSASPRMEPRAPWVEQEG PEYWEEETRNTKAHAQTDRMNLQTLRGYYNQSEASSHTLQWMIGCDLGSDGRLIRGYE RYAYD**C**KDYLALNEDLRSWTAADTAAQISKRKSEAANVAEQRRAYLEGTCVEWLHRYLE NGKEMLQRADPPKTHVTHHPVFDYEATLRCWALGFYPAEIILTWQRDGEDQTQDVELVE TRPAGDGTFQKWAAVVVPSGEEQRYTCHVQHEGLPEPLMLRWKQGSLHHILDAQKMV WNHR
F*01:01	M**G**SHSLRYFSTAVSRPGRGEPRYIAVEYVDDTQFLRFDSDAAIPRMEPREPWVEQEGPQ YWEWTTGYAKANAQTDRVALRNLLRRYNQSEAGSHTLQGMNGCDMGPDGRLLRGYHQ HAYD**C**KDYISLNEDLRSWTAADTVAQITQRFYEAEEYAEEFRTYLEGECLELLRRYLENGK ETLQRADPPKAHVAHHPISDHEATLRCWALGFYPAEITLTWQRDGEEQTQDTELVETRPA GDGTFQKWAAVVVPSGEEQRYTCHVQHEGLPQPLILRWEQSPQPTIPIGSLHHILDAQKM VWNHR
MR1 C262S	M**R**THSLRYFRLGVSDPIHGVPEFISVGYVDSHPITTYDSVTRQKEPRAPWMAENLAPDHW ERYTQLLRGWQQMFKVELKRLQRHYNHSGSHTYQRMIGCELLEDGSTTGFLQYAYD**C**Q DFLIFNKDTLSWLAVDNVAHTIKQAWEANQHELLYQKNWLEEECIAWLKRFLEYGKDTLQ RTEPPLVRVNRKETFPGVTALFCKAHGFYPPEIYMTWMKNGEEIVQEIDYGDILPSGDGTY QAWASIELDPQSSNLYSCHVEHSGVHMVLQVPGSLHHILDAQKMVWNHR
CD1d	M**A**EVPQRLFPLRSLQISSFANSSWTRTDGLAWLGELQTHSWSNDSDTVRSLKPWSQ GTFSDQQWETLQHIFRVYRSSFTRDVKEFAKMLRLSYPLELQVSAGCEVHPGNASN NFFHVAFQ**C**KDILSFQGTSWEPTQEAPLWVNLAIQVLNQDKWTRETVQWLLNGTCP QFVSGLLESGKSELKKQVKPKAWLSRGPSPGPGRLLLVCHVSGFYPKPVWVKWMR GEQEQQGTQPGDILPNADETWYLRATLDVVAGEAAGLSCRVKHSSLEGQDIVLYWG GGGGLNDIFEAQKIEWHE
β_2m	M**I**QRTPKIQVYSRHPAENGKSNFLNCYVSGF**C**PSDIEVDLLKNGERIEKVEHSDLSFSKDW SFYLLYYTEFTPTEKDEYACRVNHVTLSQPKIVKWDRDM

329 **Table S3. A summary of open MHC-I and β_2m sequences used in the study.** Below are the protein
330 sequences for the representative alleles from each HLA supertype. Cysteine mutations are colored in red.

Peptide Name	HLA Allotype	Sequence
FITC-A01	A*01:01	FITC-KSDPIVAQY
TAMRA-TAX9	A*02:01	TAMRA-KLFGYPVYV
TAMRA-PHOX2B	A*24:02	TAMRA-KYNPIRTTF
FITC-A29	A*29:02	FITC-KLIDVFHQY
FITC-A30	A*30:01	FITC-KTFPPTEPK
FITC-B07	B*07:02	FITC-KPPIFIRRL
FITC-B08	B*08:01	FITC-KLRGRAYGL
FITC-B38	B*38:01	FITC-KHIPGDTLF
FITC-B37	B*37:01	FITC-KEDLRVSSF
FITC-B58	B*58:01	FITC-KSTLQEQIGW
FITC-B15	B*15:01	FITC-KQDIYRASYY
FITC-E01	E*01:03	FITC-KLPAKAPLL
FITC-G01	G*01:01	FITC-KYIHSANVL

331 **Table S4. A summary of the fluorophore-labeled peptides used in the study.**